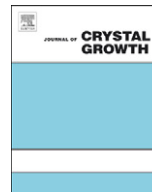




ELSEVIER

Contents lists available at ScienceDirect

Journal of Crystal Growth

journal homepage: www.elsevier.com/locate/jcrysgro

Diffusion of chromium in sapphire: The effects of electron beam irradiation

Yong-Kil Ahn, Jin-Gyo Seo, Jong-Wan Park*

Division of Materials Science and Engineering, Hanyang University, 17 Haengdang-dong, Seongdong-gu, Seoul 133-791, Republic of Korea

ARTICLE INFO

Available online 23 February 2011

Keywords:

A1. Diffusion
 B1. Chromium
 B1. Sapphire
 B3. SEM-EDX

ABSTRACT

In this paper, we measured the diffusion of chromium in sapphire (α -Al₂O₃). Sapphires were irradiated with 10 MeV electrons to fluencies of $2 \times 10^{17} \text{ cm}^{-2}$ for 1 h. Annealing experiments were performed using the three sapphire samples prepared using the three different diffusion methods at temperatures ranging from 1773 to 1923 K for 200 h under an oxidation condition of 1 atm. The diffusion of chromium in sapphire was profiled using scanning electron microscope-energy dispersive X-ray spectrometry (SEM-EDX). The following Arrhenius equations for the diffusion coefficient of Cr³⁺ were obtained over the temperature range of 1773–1923 K:

Coated and electron beam-irradiated sapphire samples,

$$D_{\text{Cr}} = 1.8 \times 10^{-7} \exp(-385.7 \pm 18.2 \text{ kJ mol}^{-1} / RT) \text{ m}^2 \text{ s}^{-1};$$

Electron beam-irradiated sapphire samples,

$$D_{\text{Cr}} = 3.3 \times 10^{-7} \exp(-401.0 \pm 14.7 \text{ kJ mol}^{-1} / RT) \text{ m}^2 \text{ s}^{-1};$$

Natural non-irradiated sapphires,

$$D_{\text{Cr}} = 2.8 \times 10^{-7} \exp(-405.9 \pm 28.7 \text{ kJ mol}^{-1} / RT) \text{ m}^2 \text{ s}^{-1}$$

These results indicate that chromium penetrated deepest within the coated and electron beam-irradiated sapphire samples.

© 2011 Elsevier B.V. All rights reserved.

1. Introduction

Different impurities in corundum (α -Al₂O₃) produce different color varieties. All colors of corundum are referred to as sapphire, except for the red color, which is known as ruby. Corundum has a trigonal lattice D_{3d}⁶ structure. The crystals have an approximately hexagonal closed packing structure of oxygen and metal atoms. The six oxygen ions are octahedrally coordinated cations; and only two-thirds of the octahedral sites are filled [1]. If corundum has more than 1000 ppm Cr³⁺ ions as impurities, it is referred to as a ruby. Rubies can be used in solid-state lasers [2], and they fetch high prices in gem markets. Chromium can be substituted for the aluminum in corundum and is present as chromium oxide. The Cr³⁺ ion is slightly larger than Al³⁺; therefore, it naturally enters easily into the corundum structure. As a result, Cr³⁺ ions form 3d³, with only three unpaired electrons in the 3d orbitals. If the Cr³⁺ ion is located in the Al³⁺ site in corundum, it coordinates the six

oxygens into a distorted octahedral configuration [3]. According to the ligand field theory [4], splitting of the 3d³(Cr³⁺) orbital should result in the spectroscopic terms ⁴A₂, ⁴T₂, ⁴T₁, and ²E. The Cr³⁺ ion has two strong absorption bands in the visible part of the spectrum, which explain the red color, i.e., 2.2 eV light can be absorbed to raise the chromium from the ⁴A₂ ground level to the ⁴T₂ excited level as absorption in the yellow-green, and 3.0 eV light raises it to the ⁴T₁ level as violet absorption. In addition, the absorption decreases to zero in the red region below 2.0 eV. Therefore, rubies have a red color with a slight purple overtone.

Our previous study on the diffusion of Cr³⁺ ions in chrysoberyl [5] verified that electron beam irradiation resulted in the deepest penetration of Cr³⁺ ions among the three methods evaluated, namely electron beam irradiation, H⁺ ion beam irradiation, and non-irradiation.

In the present study, we investigated chromium diffusion in sapphire. Furthermore, we evaluated a new method to diffuse chromium into sapphire, the uniform coating of chromium onto the surface of the sapphire using the evaporator equipment.

Our objective was to determine the optimal method for Cr³⁺ ion diffusion in a sapphire lattice. Experiments were first performed

* Corresponding author. Tel.: +82 2 2298 0386; fax: +82 2 2298 2850.
 E-mail address: jwpark@hanyang.ac.kr (J.-W. Park).

separately on pure sapphire without irradiation and subsequently on electron beam-irradiated samples and on electron beam-irradiated and coated sapphire samples. We determined the diffusion coefficients and diffusivities [$D = D_0 \exp(-Q_d/RT)$] of chromium in sapphire for all three types of sapphire samples. Finally, we analyzed the diffusion kinetics of the three samples using the activation energies obtained from the calculated diffusivities.

2. Experimental procedures

Diffusion experiments were performed on specimens of natural sapphire. The samples were colorless and free of cracks. For the coating process, 12 pieces of sapphire were sliced to a thickness of 2 mm using a diamond sawing machine. Their surfaces were smoothed using three methods in turn: silicon carbide cc-220cw, cc-2000cw abrasive paper, and alumina powder. The smoothed sapphires were cleaned in an ultrasonic bath containing distilled water for 10 min [6].

In a previous study, we found that chromium diffused deeper into chrysoberyls when using electron beams than when using proton beams for irradiation. Therefore, in the current study, we pre-irradiated sapphires in an electron accelerator at an electron energy of 10 MeV to fluencies of $2 \times 10^{17} \text{ cm}^{-2}$. Furthermore, we investigated a new method of diffusion, namely, chromium evaporation on the surfaces of sapphires followed by electron beam irradiation. Lumps of chromium metal were packed into a $1 \times 1 \times 1 \text{ cm}^3$ carbon crucible. They were melted and evaporated by the electron beam using the following conditions: beam current of 50 mA, voltage of 4.36 kV, and a high vacuum pressure of 3×10^{-6} Torr. Layers of chromium were deposited on the surface to a thickness of 1 μm . The evaporator scheme is shown in Fig. 1.

We prepared two types of chromium for diffusion: chromium oxide powder for embedding and chromium metal for use in the evaporator. For the Cr^{3+} ion doping, chromium powder (Cr_2O_3) and chromium metal of 99.0% purity were produced by Duksan Pure Chemical Co. Ltd., Korea. Experiments were performed using sapphire samples prepared using three different chromium

diffusion methods: non-irradiation, irradiation by an electron beam, and coating of the sapphire surface with chromium by an evaporator followed by irradiation with an electron beam.

To stimulate diffusion, samples were completely embedded in chromium oxide powder and were closely packed into an alumina ceramic crucible with a cover. Then, the samples were heated in an electric furnace in a horizontal alumina tube at 50 K intervals for temperatures ranging from 1773 to 1923 K for 200 h under 1 atm oxygen pressure and were annealed steadily at 3 K a minute. Samples containing diffused chromium were cut into cross-sections and were ground and polished horizontally without staining.

3. SEM-EDAX analysis

Samples were analyzed using a scanning electron microscope (SEM) (Nova Nano 200, FEI Co.). As shown in the SEM image in Fig. 2, the polished surfaces of sapphires were distinguished by Cr- and Al-rich oxide layers, along with the original interface. The highlighted line was used as the basis of line scanning for energy dispersive X-ray spectrometry (EDX). To measure the depth to which Cr^{3+} diffused in the sapphire samples, the samples were line-scanned from the highlighted line toward an aluminum-rich surface after being cross-sectioned to the center. Based on the depth profile obtained using EDX, we measured the Cr^{3+} concentration in wt%.

Fig. 3 depicts the concentration profile of Cr in sapphire samples heated at 1873 K for 200 h. The concentration profile of Cr (wt%) versus diffusion depth (μm) was consistent with a Gaussian-type distribution. The results shown in Fig. 3 were converted into $\log(\text{Cr concentration wt\%})$ versus x^2 (diffused depth), as shown in Fig. 4.

To calculate the diffusion coefficient (D), we applied Fick's second law. The concentration function of a semi-infinite system can be written as follows:

$$c(x,t) = \alpha / (\pi Dt)^{1/2} \exp(-x^2/4Dt) \quad (1)$$

This equation is a Gaussian exponential function, where $c(x,t)$ is the concentration of Cr, as functions of the diffused depth from the surface (x), the annealing time (t) and α the total amount of chromium localized on the surface of the sample ($x=0$ at

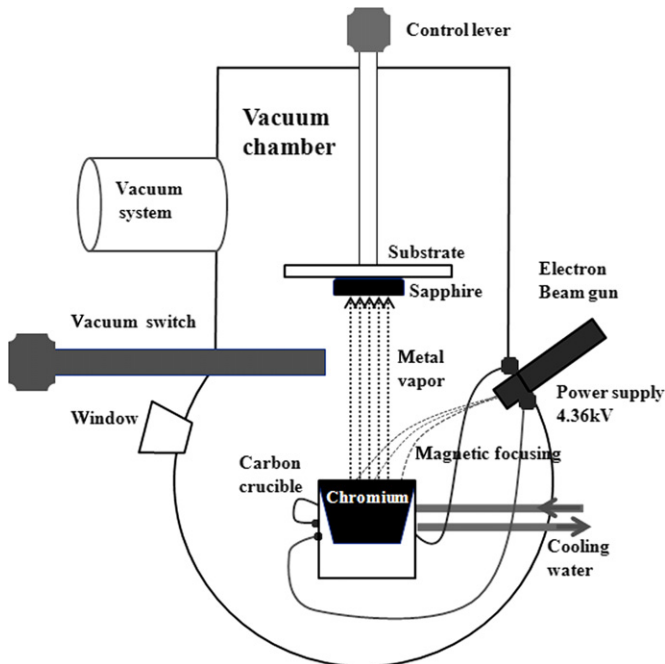


Fig. 1. Schematic illustration of the evaporator-based coating method used to coat the surfaces of sapphires with chromium.

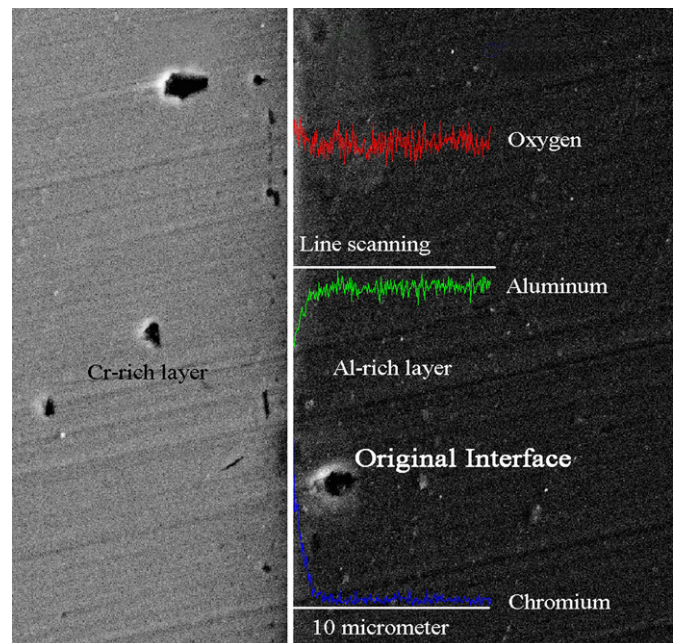


Fig. 2. Scanning electron microscope image of chromium oxide (Cr_2O_3)/sapphire (Al_2O_3) sintered under oxidation at 1873 K for 200 h.

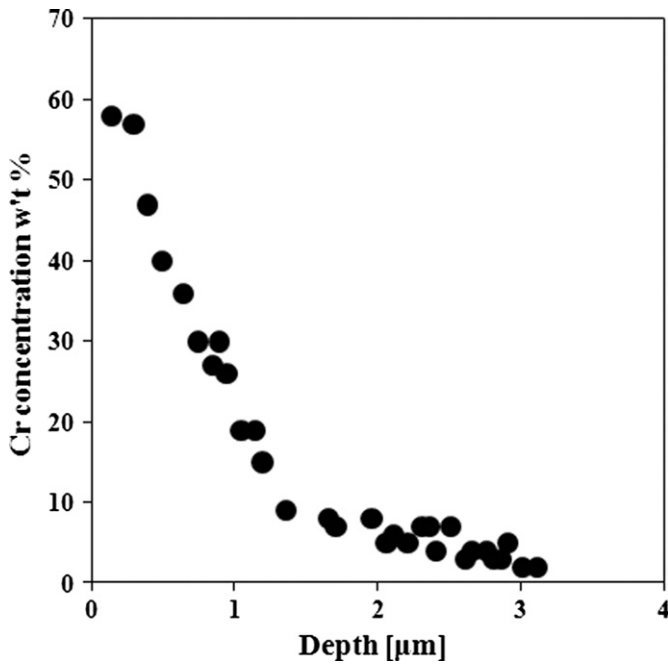


Fig. 3. Concentration profile of Cr in sapphire after annealing at 1873 K for 200 h under oxidation; a Gaussian-type dependence is evident.

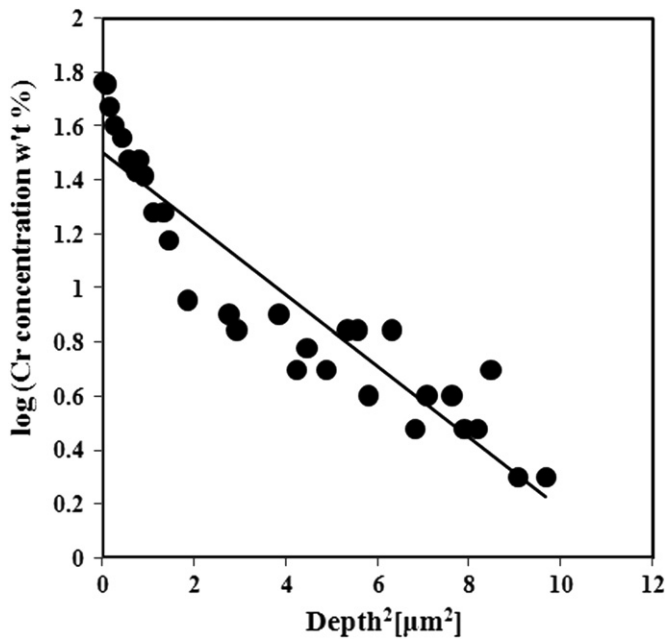


Fig. 4. Logarithm of Cr concentration versus the square of the diffused depth for the experimental data shown in Fig. 3.

$t=0$). Fig. 4 shows a simple one-dimensional function. The slope of the straight line is $-1/(2.303 \times 4Dt)$.

Therefore, the diffusion coefficient is $-1/(2.303 \times 4t \times \text{slope})$ [7]. Table 1 shows diffusion coefficients and logarithm D data for each temperature.

4. Results and discussion

Surface analysis of the sapphire samples according to SEM revealed that all of the samples had a 20–30 μm -thick layer of Cr_2O_3 crystals on their sintered surfaces. The thickness of the

Table 1
Diffusion data for Cr^{3+} in sapphire.

Sample	T (K)	$1/T$ ($10^4/\text{K}$)	T (s)	D ($\text{m}^2 \text{s}^{-1}$)	$\log D$
Non-SPC-12	1773	5.64	7.2×10^5	2.899×10^{-19}	-18.538
Non-SPC-10	1823	5.48	7.2×10^5	7.068×10^{-19}	-18.151
Non-SPC-9	1873	5.34	7.2×10^5	1.134×10^{-18}	-17.945
Non-SPC-11	1923	5.20	7.2×10^5	2.669×10^{-18}	-17.574
Ir-SPC-2	1773	5.64	7.2×10^5	5.026×10^{-19}	-18.299
Ir-SPC-5	1823	5.48	7.2×10^5	9.802×10^{-19}	-18.009
Ir-SPC-4	1873	5.34	7.2×10^5	2.111×10^{-18}	-17.676
Ir-SPC-1	1923	5.20	7.2×10^5	4.092×10^{-18}	-17.388
Co/Ir-SPC-8	1773	5.64	7.2×10^5	7.036×10^{-19}	-18.153
Co/Ir-SPC-14	1823	5.48	7.2×10^5	1.666×10^{-19}	-17.778
Co/Ir-SPC-6	1873	5.34	7.2×10^5	2.814×10^{-18}	-17.551
Co/Ir-SPC-7	1923	5.20	7.2×10^5	5.653×10^{-18}	-17.248

Cr_2O_3 powder was less than 1 μm before annealing. As shown in Fig. 5, crystals grew after annealing at 1773 and 1923 K.

To obtain activation energies and pre-exponentials, the derived diffusion coefficients were plotted against the reciprocal temperature ($1/T$), as shown in Fig. 6. The temperature had a decisive effect on the diffusion coefficients and the velocity. The temperature dependence of the diffusivity can be expressed as follows:

$$D = D_0 \exp(-Q_d/RT) \quad (2)$$

where D_0 (m^2/s) is the pre-exponential factor, Q_d (J/mol) is the activation energy, R (8.31 J/mol K) is the gas constant, and T (K) is the absolute temperature. Taking the logarithm of both sides of Eq. (2) gives

$$\ln D = \ln D_0 - Q_d/R(1/T) \quad (3)$$

Substituting common logarithms for natural logarithms gives

$$\log D = \log D_0 - Q_d/2.3R(1/T) \quad (4)$$

Eq. (4) can be expressed as a linear function of $\log D$ and $1/T$: $y = ax + b$. Therefore, the slope is equal to $-Q_d/2.3R$ and the intercept to $\log D_0$ [8].

Using the above equation, we calculated Q_d and D_0 of the coated and electron beam-irradiated, electron beam-irradiated and non-irradiated samples. Using the data shown in Table 1 and Fig. 6, Arrhenius equations for the diffusion coefficient of Cr^{3+} in the temperature range 1773–1923 K were developed for the three sample types:

Coated and electron beam-irradiated sapphires,

$$D_{\text{Cr}} = 1.8 \times 10^{-7} \exp(-385.7 \pm 18.2 \text{ kJ mol}^{-1}/RT) \text{ m}^2 \text{ s}^{-1}$$

Electron beam-irradiated sapphires,

$$D_{\text{Cr}} = 3.3 \times 10^{-7} \exp(-401.0 \pm 14.7 \text{ kJ mol}^{-1}/RT) \text{ m}^2 \text{ s}^{-1};$$

Natural non-irradiated sapphires,

$$D_{\text{Cr}} = 2.8 \times 10^{-7} \exp(-405.9 \pm 28.7 \text{ kJ mol}^{-1}/RT) \text{ m}^2 \text{ s}^{-1}$$

These results indicate that chromium diffused the deepest into the coated and electron beam-irradiated sapphire samples.

Fig. 7 shows how the Cr diffusivity measured in sapphire compares with that measured in chrysoberyl. In sapphire, Cr^{3+} ions diffused faster than they did in chrysoberyl at a temperature of 1773 K, although the diffusion rates were similar at the high temperature of 1923 K. The diffusivities of chromium in electron beam-irradiated sapphire (b) and chrysoberyl (d) were similar. The slope of diffusivity was slightly lower in sapphire than it was in chrysoberyl (Table 2), suggesting that the activation energy for diffusion of chromium in sapphire is lower than that in chrysoberyl, and that diffusion of chromium, therefore, occurs more easily in sapphire. The diffusions of atoms in different structures

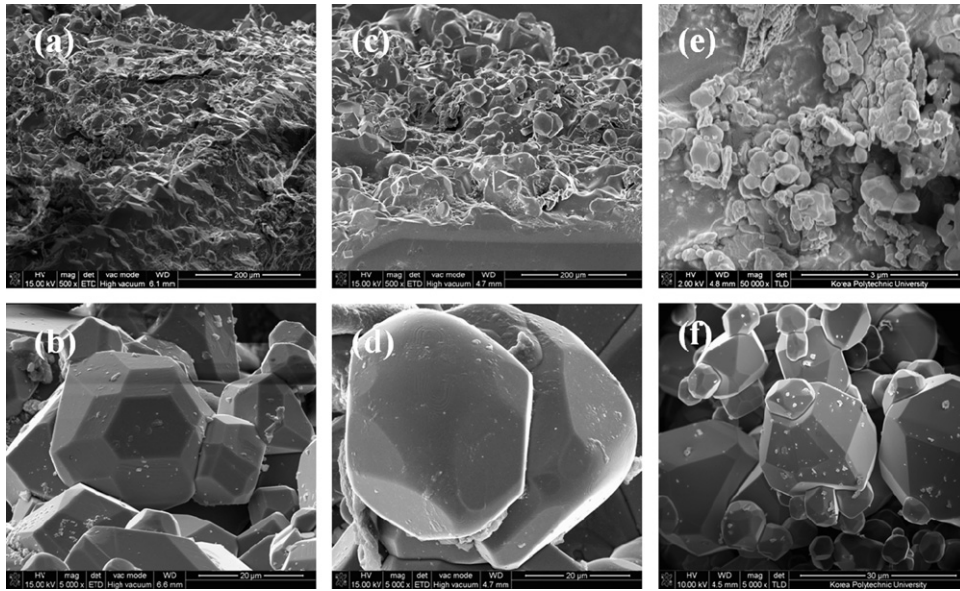


Fig. 5. SEM images of the crystal growth of chromium on the sapphire surface after sintering at 1773 K for 200 h (a) magnified 500 \times and (b) magnified 5000 \times and after sintering at 1923 K for 200 h (c) magnified 500 \times and (d) magnified 5000 \times . SEM images of (e) Cr_2O_3 powder before heating (magnified 50000 \times) and (f) Cr_2O_3 powder after heating (magnified 5000 \times).

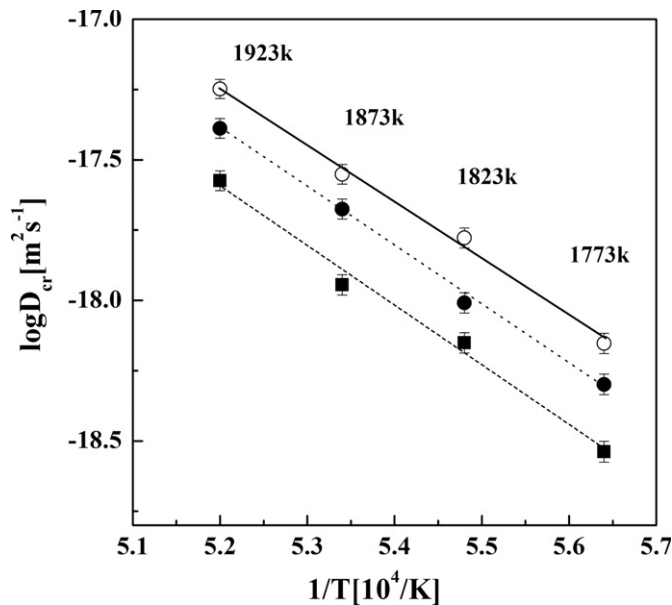


Fig. 6. Arrhenius plots of Cr diffusion in sapphire samples annealed during oxidation at temperatures from 1773 to 1923 K for 200 h. Samples coated with chromium and then irradiated with an electron beam are shown by empty circles, samples irradiated with an electron beam are shown by filled circles, and pristine, untreated samples are indicated by black squares.

are influenced by composition, stoichiometry, temperature, and pressure. In particular, porosity, site energy and ionic radius are strong determinants of diffusivity [9]. Chrysoberyl (BeAl_2O_4) and corundum ($\alpha\text{-Al}_2\text{O}_3$) are hexagonal closed packing structures. However, chrysoberyl and corundum have a trigonal and an orthorhombic structure, respectively. Furthermore, the Al^{3+} ions in corundum are octahedrally coordinated by the oxygen ions, while, in chrysoberyl, the Be^{2+} ions are additionally tetrahedral at the interstitial sites [10]. Therefore, diffusion of chromium in chrysoberyl is structurally more difficult than that in corundum.

Photoluminescence spectrum was measured to investigate the effects of electron beam irradiation on the samples. That was collected using 325 nm He–Cd laser of Kimmon Koha Co. with

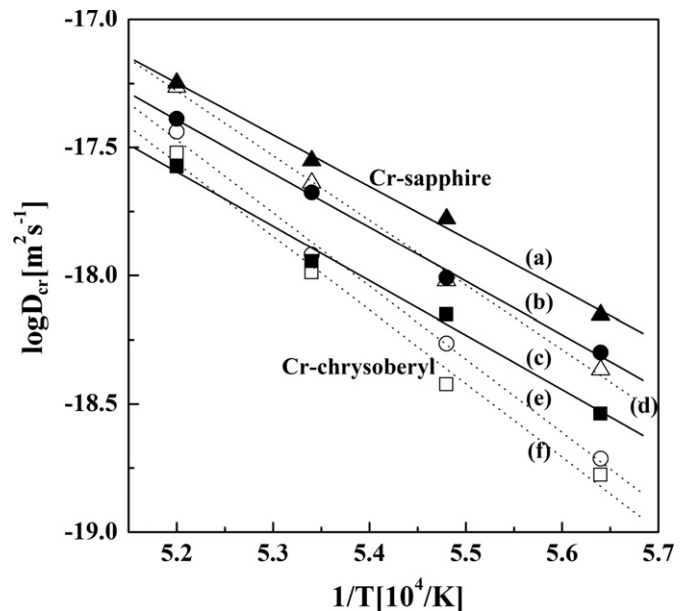


Fig. 7. Plot of Cr diffusions in sapphires (solid lines) and chrysoberyls (dotted lines). Dotted lines are Arrhenius relations from Y.K. Ahn et al. [5] for Cr diffusion in chrysoberyl. (a) Coated and electron beam-irradiated sapphire, (b) electron beam-irradiated sapphire, (c) non-irradiated sapphire, (d) electron beam-irradiated chrysoberyl, (e) proton beam-irradiated chrysoberyl, and (f) non-irradiated chrysoberyl.

Table 2

The slopes of diffusivity in sapphires and chrysoberyls.

Conditions for diffusion of chromium	Value	Error
Coated for electron beam-irradiated sapphires	-2.018	± 0.095
Electron beam-irradiated sapphires	-2.098	± 0.077
Natural non-irradiated sapphires	-2.124	± 0.150
Electron beam-irradiated chrysoberyls	-2.524	± 0.095
Proton non-irradiated chrysoberyls	-2.854	± 0.131
Natural non-irradiated chrysoberyls	-2.867	± 0.193

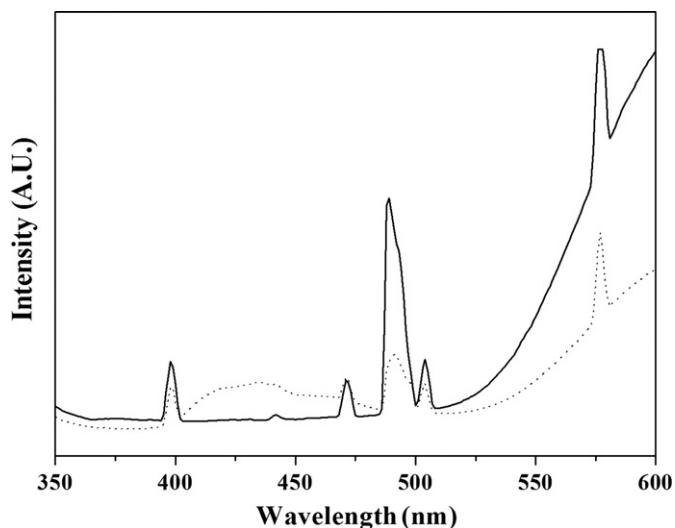


Fig. 8. Photoluminescence results for the samples using a 325 nm He–Cd excitation source. The dotted line indicates pristine material, while the solid line indicates material irradiated with a 10 MeV electron beam of $2 \times 10^{17} \text{ cm}^{-2}$ for 1 h.

Acton Co. Spectropro 2300i detector at room temperature. Photoluminescence peaks for irradiated samples are shown in Fig. 8. We noticed that samples irradiated with electron beams had far higher peak intensities than did the non-irradiated samples.

If electron energy of 10 MeV is used to irradiate samples, the penetration depth will increase linearly up to 15 mm [11]. However, to penetrate 10 mm into the sample, over 45 MeV of proton energy must be used for irradiation [12]. In a previous study, we discussed in detail the diffusion coefficients obtained using electron energy versus proton energy. Electron beam irradiation creates many cation and anion vacancies in the crystal lattice because after the primary knock-on atom receives energy from the irradiated electron, it collides with the next atom, and the subsequent atomic collisions spread widely and randomly within the crystal lattice.

If the energy is provided by an electron beam, defect centers will be changed in the crystal lattice. If there is an aluminum vacancy with a hole trapped at the adjacent oxygen when an electron of the outermost orbital leaves the oxygen ion, it will develop a new V^{2-} center. Furthermore, the electron that leaves the oxygen ion enters another oxygen vacancy, resulting in the formation of F -centers. This process allows deeper penetration into the crystal lattice as Cr^{3+} ions enter the aluminum vacancies. If the sapphire samples are heated in the presence of Cr_2O_3 powder under oxidizing conditions at high temperature, the diffused depth will be related to the number of cation and anion vacancies. It is obvious that the electric charge becomes neutral as entering Cr^{3+} ions diffuse into cation vacancies filled by electrons.

In non-irradiated samples, the crystal lattices are more stable than are the irradiated cases because fewer V^{2-} centers exist; therefore, fewer Cr^{3+} ions will enter into the sapphire lattice compared to those in the irradiated samples [13].

In addition, we investigated a new method for coating the surfaces of samples; we evaporated chromium metal uniformly on the surface of the sapphires for deeper diffusion. Even coating of chromium ensured that it entered more easily into the crystal lattice. Oxidation allowed the chromium to enter into aluminum vacancies of sapphire in the form of a Cr^{3+} ion capable of octahedrally coordinating the adjacent oxygens.

5. Conclusions

In this study, we evaluated chromium diffusion in sapphire using samples prepared in three ways (i.e., coating sapphires with chromium followed by electron beam irradiation, electron beam irradiation without coating, and non-irradiation without coating). The Arrhenius diffusivities for the three sample cases were plotted. We found that chromium penetrated deepest into the coated and electron beam-irradiated sapphire samples, followed by the electron beam-irradiated only samples, and then the non-irradiated samples.

Samples irradiated with an electron beam showed higher peak intensities than those of non-irradiated samples using photoluminescence spectrometry. This indicates the presence of more anion and cation vacancies in irradiated sapphire crystals. Therefore, samples irradiated by electron beams should show deeper diffusion of chromium compared with that of the non-irradiated samples. Indeed, in this study, sapphires coated with chromium using an evaporator showed deeper diffusion of chromium than did samples that were not coated after irradiation. Even coating of the sapphire surface with chromium therefore enhances diffusion.

To sinter the surfaces of sapphire samples containing diffused chromium, temperatures from 1773 to 1923 K are required, similar to those needed in chrysoberyl. To produce rubies from the sapphire via chromium diffusion, however, greater quantities of Cr^{3+} ions must diffuse into the surface than were recorded in our experiments. Therefore, because temperature is the limiting factor, hydrothermal methods for increasing the pressure should be investigated in future studies.

References

- [1] F. Werfel, O. Brummer, *Phys. Spr.* 28 (1983) 92.
- [2] M. Soukieh, B.A. Ghani, M. Hammadi, *Opt. Lasers Eng.* 41 (2004) 177.
- [3] K. Nassau, *The Physics and Chemistry of Color*, Wiley, New York, 1983.
- [4] B.N. Figgis, M.A. Hitchman, *Ligand Field Theory and its Applications*, New York, Wiley, 2000.
- [5] Y.K. Ahn, J.G. Seo, J.W. Park, *J. Cryst. Growth* 311 (2009) 3943.
- [6] J.M. Rickman, H.M. Chan, M.P. Harmer, *J. Am. Ceram. Soc.* 90 (2007) 1551.
- [7] F. Adam, B. Dupre, K. Kowalski, C. Gleitzer, J. Nowotny, *J. Phys. Chem. Solids* 56 (1995) 1063.
- [8] W.D. Callister Jr., *Materials Science and Engineering An Introduction*, seventh ed., Wiley, New York, 2007.
- [9] E. Dowty, *Am. Mineral.* 65 (1980) 174.
- [10] E.F. Farrell, J.H. Fang, R.E. Newnham, *Am. Mineral.* 48 (1963) 804.
- [11] B. Campbell, A. Mainwood, *Phys. Status Solidi A* 181 (2009) 99.
- [12] E.H. Kim, Y.J. Kong, D.H. Lee, H.S. Kim, J.W. Hyun, S.J. Noh, *J. Korean Phys. Soc.* 48 (2006) 860.
- [13] K.H. Lee, J.H. Crawford Jr., *Phys. Rev. B* 15 (1980) (1977) 4065.